

Heterogeneity in susceptibility dictates the order of epidemiological models

Christopher Rose,¹ Andrew J. Medford,² C. Franklin Goldsmith,¹
Tejs Vegge,³ Joshua S. Weitz,^{4,*} and Andrew A. Peterson^{1,3,†}

¹*School of Engineering, Brown University, Providence, Rhode Island, 02912, USA*

²*School of Chemical & Biomolecular Engineering,
Georgia Institute of Technology, Atlanta, Georgia, 30332, USA*

³*Department of Energy Conversion and Storage,
Technical University of Denmark, 2800 Kgs. Lyngby, Denmark*

⁴*School of Biological Sciences, Georgia Institute of Technology, Atlanta, Georgia, 30332, USA*

The fundamental models of epidemiology describe the progression of an infectious disease through a population using compartmentalized differential equations, but do not incorporate population-level heterogeneity in disease susceptibility. We show that variation leads to the natural emergence of a power law in the force of infection (βIS^p), where the order p is a simple function of the distribution shape. p is significantly greater than one for reasonable variances, suggesting that conventional epidemic models make extreme assumptions about the absence of variance in susceptibility. The power-law behavior fundamentally alters predictions of the long-term infection rate, and suggests that first-order models that are parameterized in the exponential-like phase may systematically and significantly over-estimate the final severity of the outbreak.

Mathematical models of disease dynamics divide a population into categories based on disease status; *e.g.*, susceptible (S), infectious (I), and recovered/removed (R). In the basic SIR model, the dynamics of individuals in each disease compartment can be written as¹

$$\begin{aligned} \frac{dS}{dt} &= -r_I \\ \frac{dI}{dt} &= r_I - r_R, \end{aligned} \quad (1)$$

such that $S + I + R = 1$. The Kermack–McKendrick² formulation—the basis for conventional, modern epidemiology models—assumes rates of infection and recovery to be $r_I = \beta IS$ and $r_R = \gamma I$, respectively, with β and γ taken as rate constants with dimensions of inverse time. These simplified models provide epidemiologists and policymakers with valuable intuition on the progression of an outbreak, and form the basis for more complex models that include such effects as geography, travel, latency, susceptibility to re-infection, stochasticity, and vital dynamics.^{3,4}

The SIR model assumes homogeneity of risk, an assumption unlikely to hold in practice. That is, a real population will have a distribution of susceptibilities which can be based on a mixture of behavioral attributes (such as the number of people encountered in a typical day or interaction modalities) and inherent attributes (such as age, immune status, or genetic differences).^{5–8} Empirical studies suggest that variations in susceptibility roughly follow the “80:20 rule”, with 20% of individuals carrying 80% of the collective risk.⁹ If there is variation, then individuals that are more susceptible should tend to be infected earlier, leading to changes in the susceptibility distribution. As a result, the most susceptible individuals will be disproportionately removed from the pool at the early stages of an outbreak, so that not just the *number* of people in the susceptible pool will decrease, but also

the *average susceptibility* of the pool will decrease, both of which should slow the rate of spread of the disease.

One way to incorporate variability into the SIR model is to directly account for susceptibility in the rate equations. Other epidemic models have incorporated such variability by explicitly accounting for assortative mixing,¹⁰ or variation in contacts,¹¹ or implicitly structured a population based on variation in susceptibility.¹² These analyses make different assumptions about the link between variation in risk and disease dynamics. Despite the use of different assumptions, all of these models suggest that variation in the risk of transmission can lower the herd immunity threshold (*i.e.*, the fraction of the population that must become immune for the disease to decrease in prevalence) when compared to predictions from equivalent homogeneous mixing models. This agreement suggests it may be possible to develop a unified framework to understand the joint dynamics of disease and susceptibility.

Here, we define an individual’s infection susceptibility, ε , such that individuals with $\varepsilon=2$ will become infected at twice the rate, on average, as individuals with $\varepsilon=1$, given they exist in the same population of infected people. This definition is generic, and captures heterogeneity due to behavioral and/or inherent factors. Here, we confine our analysis to the simplest case where individuals have a static susceptibility, noting that dynamic changes in behavior can be accounted for separately.¹³ If the distribution of susceptibilities in a population is given by $n_S(\varepsilon, t)$; then the infection rate is distributed as

$$\hat{r}_I(\varepsilon, t) = \beta I \varepsilon \frac{n_S(\varepsilon, t)}{N_{\text{total}}} \propto \varepsilon \cdot n_S(\varepsilon, t), \quad (2)$$

where N_{total} is the total number of individuals in the population. This distribution, which we refer to as the “draw probability” is shown with an exponential susceptibility distribution in Figure 1A–B, where it is apparent that the mean of the draw probability is higher

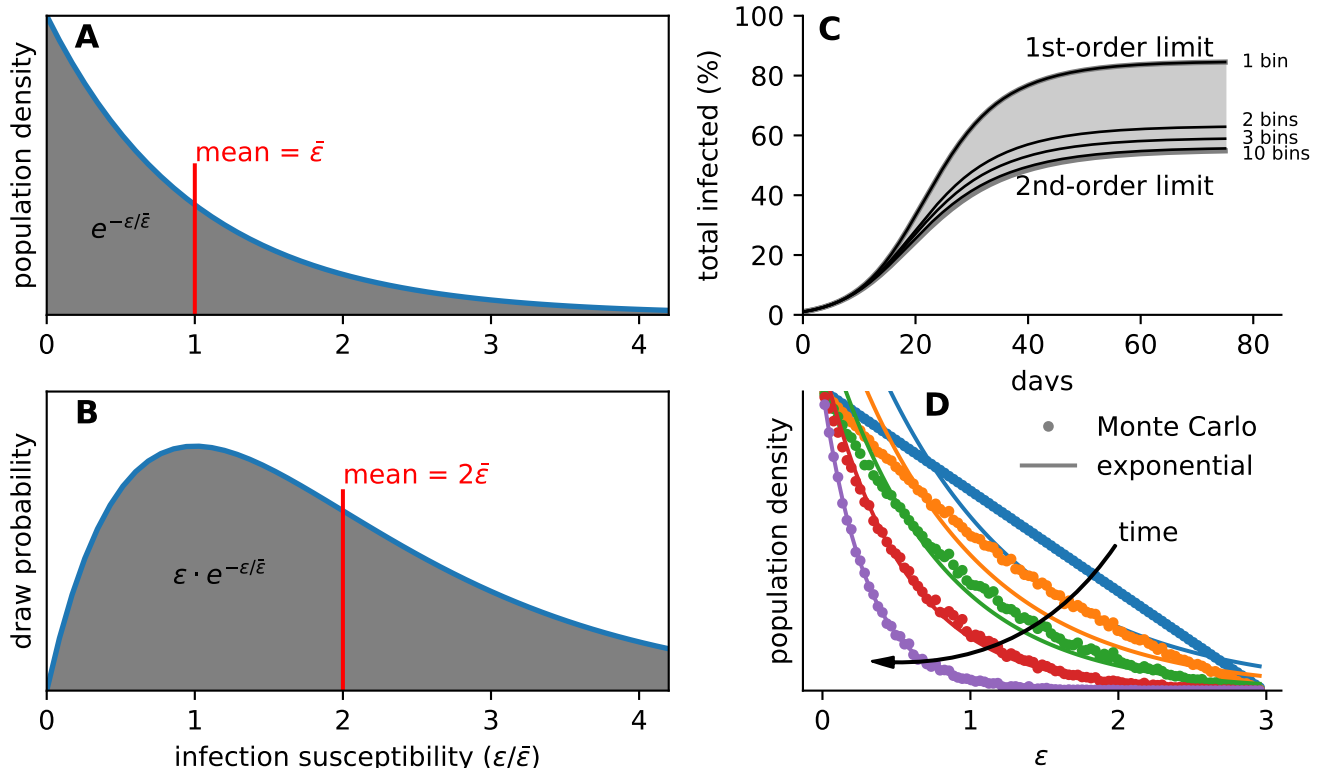


FIG. 1: **A** and **B** show a continuous distribution of infection susceptibility in a population and the probability of the next individual infected, respectively. For an exponential distribution, the mean of the lower curve is double the mean of the upper curve. **C** compares numerically integrating a 1st- and 2nd-order SIR model with that obtained from binning the susceptibility into discrete levels consistent with an initially-exponential distribution. **D** shows that an exponential distribution emerges when stochastically sampling from an initially linear distribution. The solid lines are exponential curves with the same mean as the Monte Carlo points of the same color.

than the mean of the susceptible pool. This will be true of *any* (non-singular) population distribution, putting downward pressure on the mean. The overall rate of new infections at any time is then

$$r_I = \int_0^\infty \beta I \epsilon \frac{n_S(\epsilon, t)}{N_S} d\epsilon = \beta I \bar{\epsilon} S, \quad (3)$$

where $\bar{\epsilon}(t)$ is the mean susceptibility of the pool, since $\bar{\epsilon}(t) = \frac{1}{N_S} \int_0^\infty \epsilon n_S(\epsilon, t) d\epsilon$ with N_S as the total number of susceptible people in the population. This rate form ($\beta \bar{\epsilon} I S$) is general; for example, if the entire population has an identical susceptibility of $\epsilon=1$, the above equation simplifies to the classic SIR rate.

A natural starting point is to assume that susceptibility follows a maximum-entropy distribution; *i.e.*, the least-informative default, which for positive values with a specified mean is the exponential distribution¹⁴

$$\frac{n_S(\epsilon, t)}{N_S} = \frac{e^{-\epsilon/\bar{\epsilon}(t)}}{\bar{\epsilon}(t)}.$$

For this distribution, the draw probability has a mean value of $2\bar{\epsilon}(t)$ (at any time, provided the distribution remains exponential); that is, the average individual who

gets sick was twice as susceptible as the susceptible population as a whole. (All derivations and assumptions not explicitly detailed in this manuscript are contained in the SI.) We can then express how the pool's average susceptibility $\bar{\epsilon}$ is affected by the removal of high- ϵ individuals. Since, on average, the susceptibility of a newly infected individual is $2\bar{\epsilon}$, the pool's total susceptibility changes as $d(\bar{\epsilon} N_S)/dN_S = 2\bar{\epsilon}$. Upon integration, we find the *average* susceptibility of the pool decreases in direct proportion to the number of individuals left in the pool

$$\bar{\epsilon}(t) = S(t). \quad (4)$$

As a result, for exponentially-distributed susceptibilities, the rate of new infections becomes second order in S ,

$$r_I = \beta I S^2.$$

A similar result should be observed by “binning” the susceptibility into discrete levels and introducing a separate ODE for each susceptibility level, as has been demonstrated in previous literature.⁸ We show the results of numerically integrating such a binned system given an initially exponential susceptibility distribution in Figure 1C. As the number of discrete susceptibility levels is increased, we approach the second-order behavior predicted by this analysis.

The above analysis only holds if the distribution is expected to remain exponential throughout the course of the outbreak. Since a distribution will evolve as $\partial n_S(\varepsilon, t)/\partial t = -\beta I \varepsilon n_S(\varepsilon, t)$, then the time-course of the distribution will follow

$$n_S(\varepsilon, t) = n_S(\varepsilon, 0) \cdot e^{-\beta \mathcal{X}_I(t) \varepsilon}, \quad (5)$$

where $n_S(\varepsilon, 0)$ is the initial distribution and $\mathcal{X}_I(t) \equiv \int_0^t I dt$ is a progress variable that is monotonic with time. $\mathcal{X}_I(t)$ can be thought of as the cumulative infectious driving force. Therefore, an initially exponential distribution will evolve as

$$n_S(\varepsilon, t) = \frac{N_{\text{total}}}{\bar{\varepsilon}_0} \exp \left\{ - \left(\frac{1}{\bar{\varepsilon}_0} + \beta \mathcal{X}_I(t) \right) \cdot \varepsilon \right\},$$

where $\bar{\varepsilon}_0$ is the initial mean. That is, the distribution stays exponential with respect to ε at all times. Interestingly, we also find that many starting distributions evolve toward an exponential form under the action of contagion. This is shown for a linearly-decreasing distribution in Figure 1D, which we observed via Monte Carlo simulations to tend towards an exponential, through a stochastic sampling process consistent with the draw probability.

The gamma distribution is often used to describe variations in susceptibility.^{6–8,15} This distribution is controlled via a shape parameter k and simplifies to the exponential when $k=1$. If $k < 1$, the gamma becomes a longer-tailed distribution (such as an “80:20” distribution), and as $k \rightarrow \infty$ the distribution becomes a Dirac delta function. In published studies, k is typically less than one. Conveniently, the gamma distribution is a general solution to the differential equation governing the dynamic sampling process; this makes it an “eigendistribution” of the force of infection. That is, if a population is initially gamma-distributed it will remain gamma-distributed—with the same shape parameter k and decreasing mean—under the action of equation (5).

Next we show how a gamma distribution with shape k affects the rate equation. It can be derived that the mean susceptibility, for any given distribution, evolves as

$$\frac{d\bar{\varepsilon}}{dS} = \frac{\sigma^2}{\bar{\varepsilon} S}$$

where $\sigma^2(t)$ is the variance of the distribution. Since the variance of the gamma function is $\sigma^2(t) = \bar{\varepsilon}(t)^2/k$ and k stays constant during contagion, it follows that the mean susceptibility scales as

$$\bar{\varepsilon} = S^{1/k}$$

for an initial outbreak, giving a rate

$$r = \beta I S^{1+\frac{1}{k}}.$$

This reveals a general power-law behavior for gamma-distributed susceptibility, where the power is given by

$p = 1 + 1/k$. (Power-law behavior has been suggested elsewhere in models of behavioral change;¹³ here, the behavior emerges naturally from the distribution.) In the case of exponentially-distributed susceptibility ($k=1$), second-order behavior emerges. A longer tail, corresponding to small values of k , can significantly increase the power; for example, the “80:20” distribution ($k \approx 0.25$) pushes the order to approximately five. It is only in the unlikely limit that all individuals are identical ($k \rightarrow \infty$) that we recover the first-order power of the classic SIR model, suggesting the standard SIR model relies on an extreme assumption about variation in susceptibility. This result provides a convenient framework for capturing the effects of heterogeneous susceptibility through a single additional power-law parameter, which is dictated by the variability of susceptibility.

How does the power-law dependence of the infection rate affect epidemic model predictions? First, we note that in the early, exponential-like growth phase of an outbreak—when most of the pre-emptive measures are decided—the models are indistinguishable (since $S \approx 1$). This means that when the model parameters are fit in this exponential-like growth phase, the estimates of β and γ (or alternatively $\mathcal{R}_0 \equiv \beta/\gamma$) will be identical in each model (see Figure 2A). A deviation in the dynamics of the different models appears given sufficient depletion of susceptibles (see Figure 2B). Assuming the epidemic proceeds in a naïve population, the predicted herd-immunity threshold is

$$p_C = 1 - \left(\frac{\gamma}{\beta} \right)^{k/(k+1)} = 1 - \mathcal{R}_0^{-1/p}.$$

Figure 2B shows that there can be very substantial differences between final size predictions when comparing the conventional SIR model with predictions from models with intrinsic variation in susceptibility. We note that these results agree with predictions made elsewhere that heterogeneity reduces the predicted severity of the outbreak.^{10–13} Additional final-size equations for the various scenarios are shown in the SI. The herd-immunity and final-size analyses are only meaningful when the population’s immunity is accrued naturally through the dynamics of the outbreak itself; if immunity is acquired through random immunizations, then the final size estimates will tend toward the classic SIR predictions.

Differences in final size predictions when including susceptibility as compared to those from conventional SIR models can be relevant to real-world outbreaks. We parameterized the models with the mean \mathcal{R}_0 estimated at the early stages of the 2009 H1N1 influenza outbreak, where initial estimates of the final outbreak size were reportedly much higher than occurred in practice.¹⁷ In the included bar chart (Figure 2C), we compare the model predictions using 78 published estimates¹⁶ of \mathcal{R}_0 (from different locales) to final-size measurements based on 11 serological studies.¹⁷ We observe that the higher-order models are more consistent with the final size measurements. It is not uncommon for models to over-predict

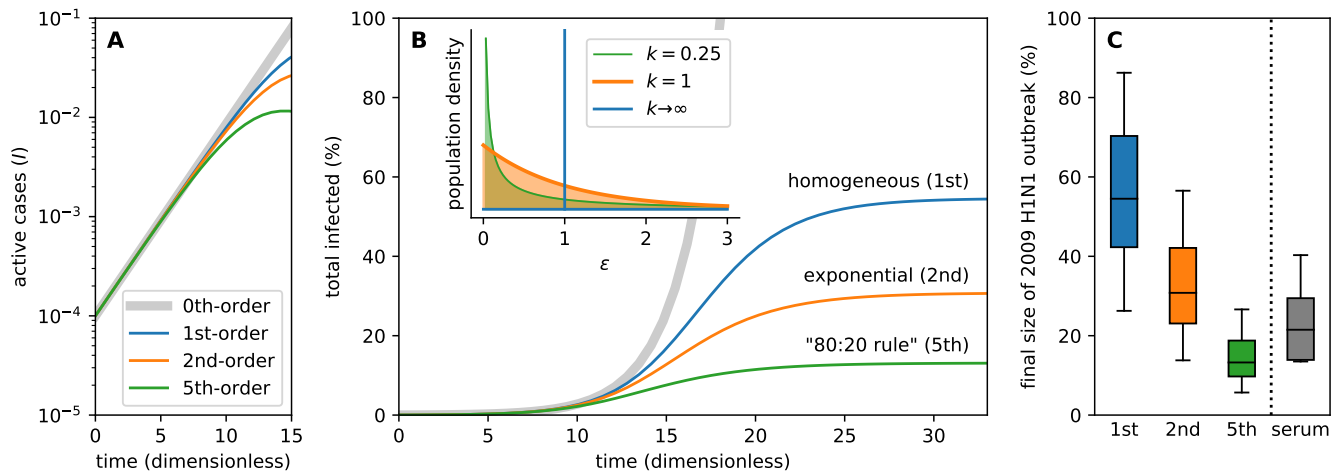


FIG. 2: **A:** The higher-order models are indistinguishable from one another in the early, exponential-like region (marked as “0th-order”), where the models are frequently parameterized. **B:** The time evolution with various assumed susceptibility distributions. The inset shows a gamma distribution at different k values. In all models, $\beta/\gamma (= \mathcal{R}_0)$ is set to 1.47, the median value estimated from 78 studies at the early stages of the 2009 H1N1 outbreak,¹⁶ and time is non-dimensionalized by the recovery rate ($\gamma \cdot t$). **C:** Final size predictions based on the 78 \mathcal{R}_0 values measured¹⁶ at early stages of the infection, in the 1st-, and 2nd-, and 5th-order models, compared with 11 seroepidemiological measurements obtained¹⁷ after the outbreak stabilized.

the ultimate size of epidemics,^{17–19} although we note that non-pharmaceutical interventions such as social distancing can also reduce this final size.^{1,20} While predicting final outbreak sizes based on initial measurements is challenging, the significant improvement of the higher-order models lends credence to the importance of accounting for heterogeneity in the susceptibility of naïve populations.

Heterogeneous variation in risk may be relevant to understanding the dynamics of COVID-19. In Figure 3 we show model predictions of an SEIR (with E indicating an exposed compartment) model using recently published²¹ parameters for the COVID-19 outbreak given $\mathcal{R}_0=2.2$ and 2.6. The traditional model predicts a much larger ultimate size and herd-immunity threshold than do the models that account for variability (with an exponential or 80:20 distribution). We caution that such predictions represent a qualitative estimate of the potential impacts of susceptibility variation on COVID-19 dynamics. Detailed integration of such an approach would require accounting for large-scale non-pharmaceutical interventions as well as detailed behavior and mixing models; however, the simple power-law rate form lends itself to integration in such models. Moreover, even the lower estimates of final size ($\sim 25\%$) suggest massive casualties ($\sim 9M$) at a global scale, using a conservative estimate²² of the infection fatality ratio of 0.5%.

There are other factors worth considering in this analysis. First, this framework does not assume any correlation between spreading propensity and infection susceptibility, so that super-spreaders appear with a frequency identical to their prevalence in the population. It seems plausible that many of the social traits that contribute to

higher susceptibility would also lead to higher spreading. If a positive correlation exists between spreading and susceptibility, then the “super-spreaders” will be most active at the beginning of an outbreak and contribute disproportionately to the rate of infection, but as the outbreak progresses, they also will be disproportionately removed early, causing more downward pressure on the relative rate of infection. The analysis also assumes that the susceptibility of each individual in the population is static over the timescales relevant to the outbreak, so that an individual does not become more or less susceptible at any point, and that there is no societal response. If these changes to susceptibility are random, this would decrease the effect suggested here; however, if they are behavior responses, it may increase the effect.¹³

Overall, this study outlines that quantifying and accounting for variability in susceptibility are critical to designing effective policies. When we account for heterogeneity in infection susceptibility, the rate equation of the standard SIR model follows a generic power law with an exponent that increases with the variance and tends toward second-order behavior for an exponential susceptibility distribution. This provides a mathematically elegant route to account for variability in human populations that are implicitly neglected in classic epidemiological models. The new framework adds negligible computational cost, facilitating integration with more complex models. More critically, the analysis reveals that assessing the joint dynamics of the susceptibility distribution can have drastic consequences on naturally-acquired herd immunity predictions, highlighting the importance of quantifying susceptibility variance for COVID-19 and other infectious diseases.

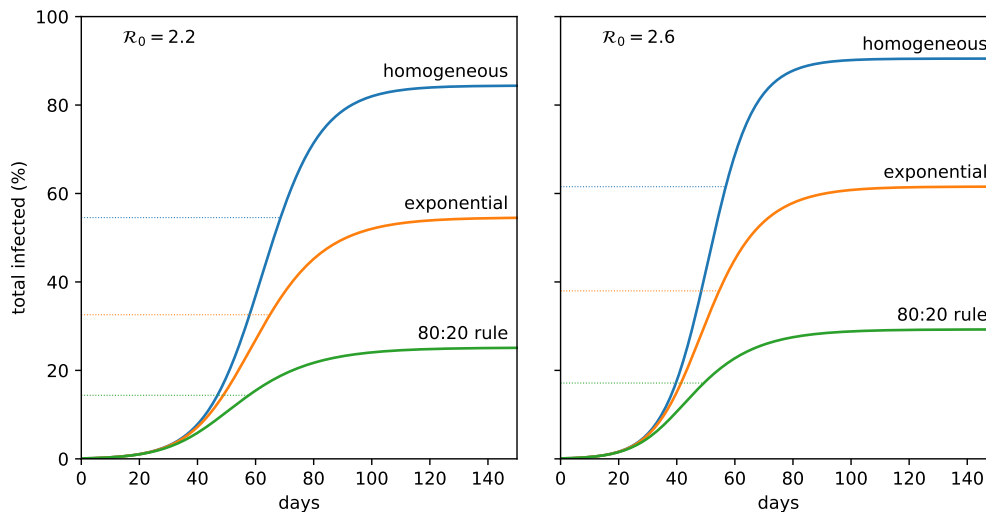


FIG. 3: SEIR (susceptible–exposed–infectious–recovered) model for the COVID-19 pandemic under different assumed susceptibility distributions, using rate parameters from Kissler *et al.*²¹ Herd immunity thresholds are indicated by the dashed lines. The parameters used were $\gamma = 1/(5 \text{ days})$ and $\delta = 1/(4.6 \text{ days})$, where γ and δ are the rates of recovery and conversion of exposed to infectious, respectively. Full details in the SI.

* jsweitz@gatech.edu

† andrew.peterson@brown.edu

¹ Bjørnstad, O.N.; Shea, K.; Krzywinski, M.; Altman, N. Modeling infectious epidemics. *Nature Methods* **2020**; *17*, 455–456.

² Kermack, W.O.; McKendrick, A.G. A contribution to the mathematical theory of epidemics. *Proceedings of the Royal Society of London. Series A, Containing Papers of a Mathematical and Physical Character* **1927**; *115*, 700–721.

³ Anderson, R.M.; May, R.M. *Infectious Diseases of Humans: Dynamics and Control*. Oxford University Press **1992**.

⁴ Keeling, M.J.; Rohani, P. *Modeling Infectious Diseases in Humans and Animals*. Princeton University Press, 1st edition **2007**.

⁵ Woolhouse, M.E.J.; Dye, C.; Etard, J.F.; Smith, T.; Charlwood, J.D.; Garnett, G.P.; Hagan, P.; Hii, J.L.K.; Ndhlovu, P.D.; Quinnell, R.J.; Watts, C.H.; Chandiwana, S.K.; Anderson, R.M. Heterogeneities in the transmission of infectious agents: Implications for the design of control programs. *Proceedings of the National Academy of Sciences* **1997**; *94*, 338–342.

⁶ Dwyer, G.; Elkinton, J.S.; Buonaccorsi, J.P. Host Heterogeneity in Susceptibility and Disease Dynamics: Tests of a Mathematical Model. *The American Naturalist* **1997**; *150*, 685–707.

⁷ Smith, D.L.; Dushoff, J.; Snow, R.W.; Hay, S.I. The entomological inoculation rate and *Plasmodium falciparum* infection in African children. *Nature* **2005**; *438*, 492–495.

⁸ King, J.G.; Souto-Maior, C.; Sartori, L.M.; de Freitas, R.M.; Gomes, M.G.M. Variation in *Wolbachia* effects on *Aedes* mosquitoes as a determinant of invasiveness and vectorial capacity. *Nature Communications* **2018**; *9*, 1483.

⁹ Corder, R.M.; Ferreira, M.U.; Gomes, M.G.M. Modelling the epidemiology of residual *Plasmodium vivax* malaria

in a heterogeneous host population: A case study in the Amazon Basin. *PLOS Computational Biology* **2020**; *16*, e1007377.

¹⁰ Britton, T.; Ball, F.; Trapman, P. A mathematical model reveals the influence of population heterogeneity on herd immunity to SARS-CoV-2. *Science* **2020**; In press, DOI:10.1126/science.abc6810.

¹¹ Hébert-Dufresne, L.; Althouse, B.M.; Scarpino, S.V.; Al-lard, A. Beyond R_0 : Heterogeneity in secondary infections and probabilistic epidemic forecasting. *ArXiv* **2020**; 2002.04004.

¹² Gomes, M.G.M.; Corder, R.M.; King, J.G.; Langwig, K.E.; Souto-Maior, C.; Carneiro, J.; Goncalves, G.; Penha-Goncalves, C.; Ferreira, M.U.; Aguas, R. Individual variation in susceptibility or exposure to SARS-CoV-2 lowers the herd immunity threshold. *medRxiv* **2020**; 2020.04.27.20081893.

¹³ Eksin, C.; Paarporn, K.; Weitz, J.S. Systematic biases in disease forecasting – The role of behavior change. *Epidemics* **2019**; *27*, 96–105.

¹⁴ Jaynes, E.T. *Probability Theory*. Cambridge University Press **2003**.

¹⁵ Langwig, K.E.; Wargo, A.R.; Jones, D.R.; Viss, J.R.; Rutan, B.J.; Egan, N.A.; Sá-Guimarães, P.; Kim, M.S.; Kurath, G.; Gomes, M.G.M.; Lipsitch, M. Vaccine Effects on Heterogeneity in Susceptibility and Implications for Population Health Management. *mBio* **2017**; *8*, e00796–17.

¹⁶ Biggerstaff, M.; Cauchemez, S.; Reed, C.; Gambhir, M.; Finelli, L. Estimates of the reproduction number for seasonal, pandemic, and zoonotic influenza: a systematic review of the literature. *BMC Infectious Diseases* **2014**; *14*, 480.

¹⁷ Nishiura, H.; Chowell, G.; Castillo-Chavez, C. Did Modeling Overestimate the Transmission Potential of Pandemic (H1N1-2009)? Sample Size Estimation for Post-Epidemic

- Seroepidemiological Studies. *PLoS ONE* **2011**; 6, e17908.
- ¹⁸ Butler, D. Models overestimate Ebola cases. *Nature* **2014**; 515, 18–18.
- ¹⁹ King, A.A.; de Cellès, M.D.; Magpantay, F.M.G.; Rohani, P. Avoidable errors in the modelling of outbreaks of emerging pathogens, with special reference to Ebola. *Proceedings of the Royal Society B: Biological Sciences* **2015**; 282, 20150347.
- ²⁰ Ma, J.; Earn, D.J.D. Generality of the Final Size Formula for an Epidemic of a Newly Invading Infectious Disease. *Bulletin of Mathematical Biology* **2006**; 68, 679–702.
- ²¹ Kissler, S.M.; Tedijanto, C.; Goldstein, E.; Grad, Y.H.; Lipsitch, M. Projecting the transmission dynamics of SARS-CoV-2 through the postpandemic period. *Science* **2020**; 368, 860–868.
- ²² Russell, T.W.; Hellewell, J.; Jarvis, C.I.; van Zandvoort, K.; Abbott, S.; Ratnayake, R.; Flasche, S.; Eggo, R.M.; Edmunds, W.J.; and, A.J.K. Estimating the infection and case fatality ratio for coronavirus disease (COVID-19) using age-adjusted data from the outbreak on the Diamond Princess cruise ship, February 2020. *Eurosurveillance* **2020**; 25, 2000256.

Supporting information

Heterogeneity in susceptibility dictates the order of epidemiological models

Christopher Rose, Andrew J. Medford, C. Franklin Goldsmith, Tejs Vegge, Joshua S. Weitz*, Andrew A. Peterson*

Contents

S1 Emergence of higher-order kinetics	1
S1.1 General rate form	1
S1.2 Exponentially-distributed susceptibilities	2
S1.3 General evolution of the mean susceptibility with time	3
S1.4 Gamma-distributed susceptibilities	4
S1.5 Note: instantaneous average susceptibility of those withdrawn	4
S1.6 Note: discrete susceptibility levels	5
S2 Distribution evolution	5
S2.1 Exponential distribution	6
S2.2 Gamma distribution	6
S3 Herd immunity thresholds and final-size calculations	6
S3.1 Herd immunity threshold	6
S3.2 Final-size calculations	7
S4 SEIR model	7

S1. Emergence of higher-order kinetics**S1.1. General rate form**

Here, we provide a more detailed derivation of the emergence of higher-order kinetics. We follow the classic SIR model, where the population is divided into susceptible, infectious, and recovered, and define N_S , N_I , and N_R as the number of people in each of these compartments. The fraction of the population in these compartments is S , I , and R , defined by dividing each of these numbers by the total population, N_{total} ($= N_S + N_I + N_R$). We also assume a initial epidemic [1], in which the entire population is in principle susceptible to the disease (minus the tiny fraction infected at the start of the model). We examine the initial SIR model for simplicity and transparency, and this general framework should lend itself to adaptation to more complex models.

The differential equations that describe the classic SIR model can be expressed as the coupled ordinary differential equations:

$$\frac{d}{dt} \begin{bmatrix} S \\ I \\ R \end{bmatrix} = \begin{bmatrix} -r_I \\ r_I - r_R \\ r_R \end{bmatrix}$$

where r_I and r_R are the rates of those becoming infected and recovering. Any of the three differential equations can be replaced with $1 = S + I + R$. In all cases, we will keep r_R in its standard form; that is, $r_R = \gamma I$.

We will examine how the rate of new infections is affected if there is risk heterogeneity in the population. We define an individual's infection susceptibility ε to be proportional to their instantaneous rate of becoming infected. If we assume the susceptibility is continuously distributed with a distribution given by $n_S(\varepsilon, t)$, then the rate will formally be defined as

$$\hat{r}_I(\varepsilon, t) = \beta I \varepsilon \frac{n_S(\varepsilon, t)}{N_{\text{total}}} \quad (\text{S.1})$$

$\hat{r}_I(\varepsilon, t)$ is properly a distribution of rates; a finite rate for a specific range of susceptibilities is obtained by integrating $\hat{r}_I(\varepsilon, t)$ between any two values of ε . The total rate of new infections at any point in time is then

$$r_I = \int_0^\infty \beta I \varepsilon \frac{n_S(\varepsilon, t)}{N_{\text{total}}} d\varepsilon$$

We can note that the average susceptibility of the susceptible pool can be calculated, at any time, by

$$\bar{\varepsilon} = \frac{\int_0^\infty \varepsilon n_S(\varepsilon, t) d\varepsilon}{N_S}$$

Thus, the rate of new infections simplifies to

$$\boxed{r_I = \beta I \bar{\varepsilon} S} \quad (\text{S.2})$$

where we emphasize that the mean susceptibility $\bar{\varepsilon}$ of this population can change over the course of the epidemic, consistent with the definitions of $\bar{\varepsilon}$ above.

Equation (S.2) is general and applies to any distribution—discrete, continuous, or single-valued. (For completeness, we also derive this assuming discrete susceptibilities in Section S1.6.) We also enforce that the average susceptibility is equal to one at the beginning of an outbreak, $\bar{\varepsilon}_0=1$, to ensure compatibility of the definition of $\bar{\varepsilon}$ with the classic model. (That is, we recover the classic SIR model by assuming that every individual is identically susceptible to infection; that is, when $\bar{\varepsilon}(t) = \bar{\varepsilon}_0 = 1$.) We next need to find how this value changes in response to the epidemic.

S1.2. Exponentially-distributed susceptibilities

For reasons we discuss in the text and in Section S2, a natural starting point is to choose a continuous, exponential distribution to describe the variation in infection susceptibility within the population. This distribution is given by

$$n_S(\varepsilon, t) = \frac{N_S}{\bar{\varepsilon}} \cdot e^{-\varepsilon/\bar{\varepsilon}}$$

We can verify that the total number of individuals in the distribution is N_S and that the mean of this distribution is given by $\bar{\varepsilon}$:

$$\begin{aligned} \int_0^\infty n_S(\varepsilon, t) d\varepsilon &= \frac{N_S}{\bar{\varepsilon}} \int_0^\infty e^{-\varepsilon/\bar{\varepsilon}} d\varepsilon = N_S \\ \langle \varepsilon \rangle &= \frac{\int_0^\infty \varepsilon \cdot e^{-\varepsilon/\bar{\varepsilon}} d\varepsilon}{\int_0^\infty e^{-\varepsilon/\bar{\varepsilon}} d\varepsilon} = \frac{[-(\varepsilon\bar{\varepsilon} + \bar{\varepsilon}^2) e^{-\varepsilon/\bar{\varepsilon}}]_0^\infty}{[-\bar{\varepsilon} e^{-\varepsilon/\bar{\varepsilon}}]_0^\infty} = \bar{\varepsilon} \end{aligned}$$

For convenience, we will define the total susceptibility of the population as $E \equiv N_S \cdot \bar{\varepsilon} = \int_0^\infty \varepsilon n_S(\varepsilon, t) d\varepsilon$. The average ε of a person removed from the population, at any instant in time, is found from the distribution of rates as (see note in Section S1.5 below)

$$\langle \varepsilon \rangle_{\text{removed}} \equiv \frac{\int_0^\infty \varepsilon \cdot \hat{r}_I(\varepsilon, t) d\varepsilon}{\int_0^\infty \hat{r}_I(\varepsilon, t) d\varepsilon} = \frac{[-\bar{\varepsilon} \cdot (\varepsilon^2 + 2\bar{\varepsilon}\varepsilon + 2(\bar{\varepsilon})^2) e^{-\varepsilon/\bar{\varepsilon}}]_0^\infty}{[-\bar{\varepsilon} \cdot (\varepsilon + \bar{\varepsilon}) e^{-\varepsilon/\bar{\varepsilon}}]_0^\infty} = 2\bar{\varepsilon} \quad (\text{S.3})$$

That is, the average not-yet-infected person has susceptibility of $\bar{\varepsilon}$, while the average person becoming infected has susceptibility $2\bar{\varepsilon}$. This is valid at any time, provided the population stays exponentially distributed (which, as we discuss in Section S2 is the expected behavior if the initial distribution is exponential). Therefore, the total susceptibility of the pool changes as

$$\frac{dE}{dN_S} = 2\bar{\varepsilon}$$

Since $E = \bar{\varepsilon} N_S$, it follows that $\frac{dE}{dN_S} = \bar{\varepsilon} + N_S \frac{d\bar{\varepsilon}}{dN_S}$. Combined with the previous result, we obtain:

$$\frac{d\bar{\varepsilon}}{dN_S} = \frac{\bar{\varepsilon}}{N_S}$$

which upon integration gives

$$\frac{\bar{\varepsilon}}{\bar{\varepsilon}_0} = \frac{N_S}{N_{S,0}}$$

For the case of an initial outbreak $\bar{\varepsilon}_0 = 1$ and $N_{S,0} \approx N_{\text{total}}$, so we find

$$\boxed{\bar{\varepsilon} = S} \quad (\text{S.4})$$

That is, the average susceptibility decreases in direct proportion to the fraction of the population still susceptible. Inserting this into our rate equation, (S.2), gives rise to second-order kinetics:

$$\boxed{r_I = \beta I S^2}$$

And thus, if we account for the heterogeneity of infection susceptibility in the population with an exponential distribution, the SIR model should be written as

$$\frac{d}{dt} \begin{bmatrix} S \\ I \\ R \end{bmatrix} = \begin{bmatrix} -\beta I S^2 \\ \beta I S^2 - \gamma I \\ \gamma I \end{bmatrix}$$

S1.3. General evolution of the mean susceptibility with time

The generalization of equation (S.3) for any distribution $n_S(\varepsilon, t)$ is

$$\langle \varepsilon \rangle_{\text{removed}} \equiv \frac{\int_0^\infty \varepsilon \cdot \hat{r}_I(\varepsilon, t) d\varepsilon}{\int_0^\infty \hat{r}_I(\varepsilon, t) d\varepsilon} = \frac{\int_0^\infty \varepsilon^2 n_S(\varepsilon, t) d\varepsilon}{\int_0^\infty \varepsilon n_S(\varepsilon, t) d\varepsilon} = \frac{\sigma^2 + \bar{\varepsilon}^2}{\bar{\varepsilon}} = \frac{\sigma^2}{\bar{\varepsilon}} + \bar{\varepsilon} \quad (\text{S.5})$$

where σ^2 is the variance, which for a continuous function can be written as $\sigma^2 = \int \varepsilon^2 n_S(\varepsilon, t) d\varepsilon - \bar{\varepsilon}^2$. That is, this gives the average susceptibility of those removed from the pool at any time t . By identical manipulations as in the exponential case, we can find a differential equation for how the mean susceptibility evolves with the pool size:

$$\frac{d(\bar{\varepsilon} N_S)}{dN_S} = \bar{\varepsilon} + N_S \frac{d\bar{\varepsilon}}{dN_S} = \frac{\sigma^2}{\bar{\varepsilon}} + \bar{\varepsilon}$$

$$\boxed{\frac{d\bar{\varepsilon}}{dN_S} = \frac{\sigma^2}{\bar{\varepsilon} N_S}} \quad (\text{S.6})$$

S1.4. Gamma-distributed susceptibilities

The gamma distribution, at mean $\bar{\varepsilon}$ and with shape parameter k , is written as

$$\frac{n_S(\varepsilon, t)}{N_S} = \frac{\varepsilon^{k-1} e^{-\varepsilon k/\bar{\varepsilon}}}{\left(\frac{\bar{\varepsilon}}{k}\right)^k \Gamma(k)}$$

As we show in Section S2.2, the gamma distribution is an ‘‘eigendistribution’’ of these dynamics; that is, if the initial susceptibility is gamma distributed with shape k , the distribution at all times will remain gamma-distributed with shape k (but in general with changing mean).

The variance of the gamma distribution is $\sigma^2 = \bar{\varepsilon}^2/k$, which if we use with equation (S.6) leads to

$$\int_1^{\bar{\varepsilon}} \frac{d\bar{\varepsilon}}{\bar{\varepsilon}} = \frac{1}{k} \int_{N_{\text{total}}}^{N_S} \frac{dN_S}{N_S}$$

$$\bar{\varepsilon} = S^{1/k}$$

(For an initial outbreak with naturally acquired infections.) Thus, the rate equation for gamma-distributed susceptibilities becomes a general power-law form based on the shape parameter k of the gamma distribution:

$$r_I = \beta I S^{1+\frac{1}{k}}$$

We see that when $k=1$, we recover the second-order behavior of the exponential distribution, and when $k \rightarrow \infty$ we recover the first-order model of an identically-susceptible population. The differential equations of the SIR model with gamma-distributed susceptibility is therefore:

$$\frac{d}{dt} \begin{bmatrix} S \\ I \\ R \end{bmatrix} = \begin{bmatrix} -\beta I S^p \\ \beta I S^p - \gamma I \\ \gamma I \end{bmatrix}$$

where $p = 1 + 1/k$.

S1.5. Note: instantaneous average susceptibility of those withdrawn

Here, we provide justification for equation (S.3). (Note that for simplicity, we referred to this as the ‘‘draw probability’’ in the main text; what we provide here is more rigorous.) Let’s first consider the simple case where we just have two discrete susceptibilities, ε_1 and ε_2 . The average ε of those individuals withdrawn (infected) in the time period between t and $t + \delta t$ is

$$\langle \varepsilon \rangle_{\text{removed}} = \frac{\varepsilon_1 \cdot \left(\text{number withdrawn with } \varepsilon_1 \text{ in } (t, t + \delta t) \right) + \varepsilon_2 \cdot \left(\text{number withdrawn with } \varepsilon_2 \text{ in } (t, t + \delta t) \right)}{\left(\text{number withdrawn with } \varepsilon_1 \text{ in } (t, t + \delta t) \right) + \left(\text{number withdrawn with } \varepsilon_2 \text{ in } (t, t + \delta t) \right)}$$

$$\langle \varepsilon \rangle_{\text{removed}} = \frac{\varepsilon_1 \cdot \int_t^{t+\delta t} r_1 dt + \varepsilon_2 \cdot \int_t^{t+\delta t} r_2 dt}{\int_t^{t+\delta t} r_1 dt + \int_t^{t+\delta t} r_2 dt}$$

Taking the limit as $\delta t \rightarrow 0$ gives us the instantaneous average ε of those withdrawn at time t (using L’Hôpital’s Rule and the Fundamental Theorem of Calculus):

$$\langle \varepsilon \rangle_{\text{removed}} = \frac{\varepsilon_1 r_1 + \varepsilon_2 r_2}{r_1 + r_2}$$

This can be generalized to any number of levels as

$$\langle \varepsilon \rangle_{\text{removed}} = \frac{\sum_i \varepsilon_i r_i}{\sum_i r_i}$$

In the continuum limit, the above becomes

$$\langle \varepsilon \rangle_{\text{removed}} = \frac{\int_0^\infty \varepsilon \cdot \hat{r}_I(\varepsilon, t) d\varepsilon}{\int_0^\infty \hat{r}_I(\varepsilon, t) d\varepsilon}$$

S1.6. Note: discrete susceptibility levels

Here, we show that equation (S.2)—that is $r_I = \beta \bar{\varepsilon} I S$ —also arises if we assume that the susceptibility is binned into discrete levels. If we have discrete levels of susceptibility in a population, a rate equation of new infections is written for each value of susceptibility ε_i as

$$r(\varepsilon_i) = \beta I \varepsilon_i S_i$$

where S_i is the fraction of the total population with susceptibility ε_i . The total rate of new infections at any point in time is then

$$r_I = \sum_i \beta I \varepsilon_i S_i$$

The average susceptibility of the susceptible pool can be calculated, at any time, by

$$\bar{\varepsilon} = \sum_i \varepsilon_i S_i$$

Thus, the rate of new infections again simplifies to

$$r_I = \beta I \bar{\varepsilon} S$$

S2. Distribution evolution

Here, we derive how distributions evolve in time, which in general will show that gamma-distributed functions (including the exponential distribution) will remain in the same shape through the action of contagion. Consider a population of susceptible individuals with a distribution given by $n_S(\varepsilon, t)$. The distribution will evolve according to the partial differential equation:

$$\frac{\partial n_S(\varepsilon, t)}{\partial t} = -\beta \varepsilon I n_S(\varepsilon, t)$$

Integrating at a particular value of ε gives

$$n_S(\varepsilon, t) = n_S(\varepsilon, 0) \cdot \exp \left\{ -\beta \varepsilon \int_0^t I dt \right\}$$

$$\boxed{n_S(\varepsilon, t) = n_S(\varepsilon, 0) \cdot e^{-\beta \varepsilon \mathcal{X}_I(t)}} \tag{S.7}$$

where we have defined $\mathcal{X}_I(t) \equiv \int_0^t I dt$ as a progress variable that is monotonic with time (since $I \geq 0$). This equation shows how any distribution will evolve over time under the force of contagion.

S2.1. Exponential distribution

If the original susceptibility distribution is exponential with initial mean $\bar{\varepsilon}_0$; that is,

$$n_S(\varepsilon, 0) = \frac{N_{\text{total}}}{\bar{\varepsilon}_0} e^{-\varepsilon/\bar{\varepsilon}_0}$$

then equation (S.7) gives

$$n_S(\varepsilon, t) = \frac{N_{\text{total}}}{\bar{\varepsilon}_0} \exp \left\{ - \left(\frac{1}{\bar{\varepsilon}_0} + \beta \mathcal{X}_I(t) \right) \cdot \varepsilon \right\}$$

That is, the distribution will remain exponentially distributed, with respect to ε , at all times. By inspection of the form, we can see that the mean evolves as

$$\bar{\varepsilon}(t) = \frac{1}{\frac{1}{\bar{\varepsilon}_0} + \beta \mathcal{X}_I(t)}$$

S2.2. Gamma distribution

If the original susceptibility distribution is gamma-distributed with initial mean $\bar{\varepsilon}_0$ and shape parameter k ; that is,

$$n_S(\varepsilon, 0) = N_{\text{total}} \frac{\varepsilon^{k-1} e^{-\varepsilon/\bar{\varepsilon}_0}}{\left(\frac{\bar{\varepsilon}_0}{k}\right)^k \Gamma(k)}$$

(where $\Gamma(k)$ is the gamma function) then equation (S.7) gives

$$n_S(\varepsilon, t) = N_{\text{total}} \frac{\varepsilon^{k-1} e^{-\left(\frac{k}{\bar{\varepsilon}_0} + \beta \mathcal{X}_I(t)\right)\varepsilon}}{\left(\frac{\bar{\varepsilon}_0}{k}\right)^k \Gamma(k)}$$

which is itself a gamma distribution with shape k and mean

$$\bar{\varepsilon}(t) = \frac{1}{\frac{1}{\bar{\varepsilon}_0} + \frac{\beta \mathcal{X}_I(t)}{k}}$$

That is, a gamma distribution of shape k stays a gamma distribution of shape k under the action of contagion. Thus, we can consider this an ‘‘eigendistribution’’.

Note that the exponential distribution can be expressed as a gamma distribution with shape $k = 1$.

S3. Herd immunity thresholds and final-size calculations

We emphasize that both of the results below are valid when immunity is obtained naturally; if immunity is instead obtained randomly (as may be a more appropriate assumption if immunizations are employed) then the first-order model may be a more appropriate assumption.

S3.1. Herd immunity threshold

The herd immunity threshold is defined as the fraction of the population that must be infected for the rate of new infections to go into decline. This occurs when $dI/dt = 0$ (that is, when the sign changes from positive to negative); which in the (power-law) SIR model is

$$\frac{dI}{dt} = +\beta IS^p - \gamma I = 0$$

where $p = 1 + 1/k$ for the k -shaped gamma distribution. That is, it occurs when

$$S = \left(\frac{\gamma}{\beta}\right)^{1/p} = \frac{1}{\mathcal{R}_0^{k/(k+1)}}$$

where $\mathcal{R}_0 \equiv \beta/\gamma$. The fraction of the population that must be infected is often denoted as p_C , and is therefore

$$p_C = 1 - \mathcal{R}_0^{-k/(k+1)}$$

S3.2. Final-size calculations

The predicted final size of an outbreak is the proportion of the population that is ever infected if the outbreak is allowed to proceed without intervention; [2,3] however, we note that even temporary interventions can affect the final size prediction. (That is, if \mathcal{R}_0 is temporarily reduced through non-pharmaceutical interventions that are later relaxed.) The final size is traditionally found by forming dI/dS :

$$\frac{dI}{dS} = \frac{dI}{dt} \cdot \frac{dt}{dS} = \frac{\beta IS^p - \gamma I}{-\beta IS^p} = \frac{1}{\mathcal{R}_0 S^p} - 1$$

where $\mathcal{R}_0 \equiv \beta/\gamma$ and $p = 1 + 1/k$ for the k -shaped gamma distribution. This is integrated from the beginning to the end of the outbreak:

$$\int_{I_0}^{I_\infty} dI = \int_{S_0}^{S_\infty} \left(\frac{1}{\mathcal{R}_0 S^p} - 1 \right) dS$$

where the subscripts 0 and ∞ mean the quantities are evaluated at $t=0$ and $t \rightarrow \infty$, respectively. The outbreak ends with $I_\infty = 0$; also employing $I_0 \approx 0$ and $S_0 \approx 1$ as bounds we find

$$0 = \frac{1}{1-p} \left(\frac{1}{\mathcal{R}_0 S_\infty^{p-1}} - \frac{1}{\mathcal{R}_0} \right) - S_\infty + 1 \quad (p\text{th-order})$$

$$0 = \frac{1}{\mathcal{R}_0} \ln S_\infty - S_\infty + 1 \quad (1\text{st-order})$$

A closed-form solution is available when $p = 2$. In other cases an implicit algebraic formula is provided. The final size is defined as $Z \equiv 1 - S_\infty$ giving:

$$Z = 1 - e^{-Z/\mathcal{R}_0} \quad (1\text{st-order})$$

$$Z = 1 - \frac{1}{\mathcal{R}_0} \quad (2\text{nd-order})$$

$$Z = \frac{1}{(1-p)\mathcal{R}_0} \left(1 - \frac{1}{(1-Z)^{p-1}} \right) \quad (p\text{th-order})$$

S4. SEIR model

To facilitate comparisons with recent literature, we employed an SEIR (susceptible–exposed–infectious–recovered) model with estimated parameters from the COVID-19 outbreak as published by Kissler *et al.* [4]. When incorporating the power law, this model is written as

$$\frac{d}{dt} \begin{bmatrix} S \\ E \\ I \\ R \end{bmatrix} = \begin{bmatrix} -\beta IS^p \\ +\beta IS^p - \delta E \\ +\delta E - \gamma I \\ +\gamma I \end{bmatrix}$$

where for the gamma distribution $p = 1 + 1/k$, where k is the shape parameter. Any differential equation can be replaced by the algebraic equation $S + E + I + R = 1$. The parameters taken from reference [4] are $Ro \equiv \beta/\gamma = 2.2$ or 2.6 , $\gamma = 1/(5 \text{ days})$, and $\delta = 1/(4.6 \text{ days})$.

References

- [1] Bjørnstad, O.N.; Shea, K.; Krzywinski, M.; Altman, N. Modeling infectious epidemics. *Nature Methods* **2020**; 17, 455–456.
- [2] Kermack, W.O.; McKendrick, A.G. A contribution to the mathematical theory of epidemics. *Proceedings of the Royal Society of London. Series A, Containing Papers of a Mathematical and Physical Character* **1927**; 115, 700–721.
- [3] Ma, J.; Earn, D.J.D. Generality of the Final Size Formula for an Epidemic of a Newly Invading Infectious Disease. *Bulletin of Mathematical Biology* **2006**; 68, 679–702.
- [4] Kissler, S.M.; Tedijanto, C.; Goldstein, E.; Grad, Y.H.; Lipsitch, M. Projecting the transmission dynamics of SARS-CoV-2 through the postpandemic period. *Science* **2020**; 368, 860–868.